RSC Advances

Fabrication and Properties of Polybutadiene Rubber-interpenetrating Cross-linking Poly (Propylene Carbonate) Network as Gel Polymer Electrolytes for Lithium-ion Battery

Journal:	*RSC Advances*
Manuscript ID:	RA-ART-03-2015-005276.R1
Article Type:	Paper
Date Submitted by the Author:	22-May-2015

Complete List of Authors:	Huang, Xueyan; South China Agricultural University, Institute of Biomaterial, College of Science Huang, Jiayi; South China Agricultural University, Institute of Biomaterial, College of Science Wu, jianfeng; State Key Laboratory of Motor Vehicle Biofuel Technolog, Nanyang, 473000, China, Yu, Xiaoyuan; South China Agricultural University, Institute of Biomaterial, College of Science Gao, Qiongzhi; South China Agricultural University, Institute of Biomaterial, College of Science Luo, Ying; South China Agricultural University, Institute of Biomaterial, College of Science Hu, Hang; South China Agricultural University, Institute of Biomaterial, College of Science

RSC Advances

ARTICLE

Fabrication and Properties of Polybutadiene Rubber-interpenetrating Cross-linking Poly (Propylene Carbonate) Network as Gel Polymer Electrolytes for Lithium-ion Battery

Received 00th January 20xx,
Accepted 00th January 20xx

DOI: 10.1039/x0xx00000x

www.rsc.org/

Xueyan Huang, [a] Jiayi Huang, [a] Jianfeng Wu, [b] Xiaoyuan Yu, *[a] Qiongzhi Gao, [a] Ying Luo, [a] Hang Hu** [a]

Polybutadiene rubber-interpenetrating cross-linking poly (propylene carbonate) (named as XBRPC) membrane can be readily synthesized from Polybutadiene rubber (BR), poly (propylene carbonate) (PPC), polyethylene glycol (PEG), and using benzoyl peroxide (BPO) as cross-linking agent, then actived by absorbing liquid electrolyte to fabricate a novel XBRPC gel polymer electrolyte (GPE) for lithium-ion battery. Electrolyte uptake, mechanical strength, ionic conductivity, electrochemical stability window and charge/discharge performances of the XBRPC membranes were then investigated. The results show that the XBRPC GPEs possess good mechanical strength and high electrolyte uptake. The ionic conductivity was up to 1.25 mS cm^{-1} at room temperature and 3.51 mS cm^{-1} at 80°C for XBRPC70 (70/30 of PPC/BR, w/w) sample. Furthermore, the electrochemical stability window has been established to with stand voltages greater than 4.5 V. The results of charge/discharge tests show that the initial discharge capacity of Li/ XBRPC70 GPE/ $LiFePO_4$ cell is 119 mAh g^{-1} at a current rate of 0.1C and in voltage range of 2.5-4.0V at room temperature. It also exhibited excellent cycling retention performance for high-performance lithium rechargeable battery.

Introduction

Lithium-ion batteries have been considered as a promising and clear power source for a wide variety of applications, such as energy storage systems and electric vehicles due to their high energy density and safety [1-5]. However, studies on lithium ion batteries that use liquid electrolytes have been reported to raise the possibility of explosions because of the existence of highly flammable organic liquid electrolytes [6-9]. Polymer electrolytes provide an ideal way to solve the safe problem, because of their potential application as the electrolyte in all-solid-state rechargeable lithium batteries [10].The improvement of the conductivity of gel polymeric systems is an important aspect of research activities on this field, while the solid polymer electrolyte with lowly ionic conductivity cannot meet the requirement of the rate performance. The gel polymer electrolytes (GPEs) exhibit a number of advantages, which include featuring the characteristics of both solid and liquid electrolytes, providing ionic transport at par with liquid electrolytes, being chemically compatible with electrode materials, showing acceptable ionic conductivity over a wide temperature range , possessing high thermal stability and flexibility, as well as leak free in operation [11-14]. Host polymers used for GPE preparation include poly-(ethylene oxide) (PEO) [15-16], poly(vinylidene fluoride)(PVdF) [17], poly(vinylidene fluoride-co-hexaflouropropylene) (P(VdF-HFP)) [18-19], poly(urethane) (PU) [20], poly-(acrylonitrile) (PAN) [21], and poly(methyl methacrylate) (PMMA) [22]. However, the performances of these GPEs are still unsatisfactory.

Unlike usual liquid electrolytes which are impossible to assemble without a conventional separator in a cell, the GPEs can be conveniently assembled without a film separator in a lithium-ion battery.

Poly (propylene carbonate) (PPC)-based electrolyte has been studied as solid polymer electrolyte [23] and GPEs[24] due to its good thermal properties, low cost, biodegradable properties [25] and interfacial stability with lithium metal. The ether linkage of PPC results in segment motion of the polymeric chain, which is beneficial for ionic conduction. Moreover, the ester group on the main chain of PPC is conductive to trapping liquid electrolytes. However, after soaking in the electrolyte solution, the PPC is dissolved in it and lose the mechanical strength very soon. Thus, blending with other polymers to inhibiting its dissolution is a practical solution.

In this work, we focused on improving the mechanical strength and ion conductivity of the PPC based GPEs. Butadiene rubber (BR) with a cross-linking polymeric framework as supporter was introduced to PPC to increase the mechanical strength. Additionally, BR has the advantage of being easily obtained, low prices, good mechanical strength and soft elastomeric characteristics. BR has been used as functional binder for polymer electrolytes used in lithium ion batteries [26-28]. So the addition of BR will not only enhance the elasticity of the GPEs, which results in an excellent electrode-electrolyte

[a] Institute of Biomaterial, College of Materials and Energy, South China Agricultural University, Guangzhou, 510642, China;
[b] State Key Laboratory of Motor Vehicle Biofuel Technolog , Nanyang, 473000, China
Corresponding authors, Xiaoyuan Yu, Email: yuxiaoyuan@scau.edu.cn. Hang Hu, Email: huhang@scau.edu.cn

contact, but also can lower the production cost of the GPEs. Therefore, we synthesized a composite of BR-interpenetrating cross-linked PPC network, denoted as XBRPC, where the cross-linking network was further interpenetrated by the BR to constitute a strong skeleton serve as a supporter or separator. Besides, the introduction of a small amount of polyethylene glycol (PEG) will give rise to increasing the compatibility of the nonpolar BR and the polar PPC and forming composite films with homogeneous structure. These composite films have been swelled in electrolytes solution to fabricate a novel XBRPC GPE, which exhibits high ionic conductivity, good mechanical strength, a stable electrochemical window and good thermal stability. The XBRPC GPE shows higher ionic conductivities than the commercial separator, Celgard M824 (0.45−0.90 mS cm^{-1}) [13] in the temperature range of 30-90 °C.

Experimental

Preparation of XBRPC Membrane

Poly (propylene carbonate) (PPC, average Mw = 120k supplied by henantianguan) and Butadiene rubber (BR, supplied by Thaihua Company, Tailand) were dried under vacuum at 80°C for 24 h before using. 1M $LiPF_6$ in Ethylene carbonate (EC)/ Dimethyl carbonate (DMC) (1:1, v/v) was purchased from Tinci Materials Technology Co., Ltd. Acetone (A.R.) and methylbenzene (A.R.) were purchased from Baishi Chemical Industry Co., Ltd. All the solvents were used as received without further treatment.

Different weight ratios of PPC and BR (50:50; 60:40; 70:30; and 80:20) were dissolved in a 35 cm^3 mixed solvent of acetone and methylbenzene (1:1, v/v) with 5w% of PEG and 10wt% BPO(related to weight of BR) at room temperature for 6 h under vigorous stirring to form a about 12wt% homogeneous solution, separately. According to the content of PPC, the samples were denoted as XBRPC50, XBRPC60, XBRPC70 and XBRPC80, respectively. The solutions were cast into Petri dishes with diameter of 90 mm, and most of the solvent was evaporated at room temperature to form XBRPC membrane, which were then cross-linked by a thermal pressing process in semiautomatic molding pressing machine under pressure of 10 MPa and at 100°C for 10 min. Finally the XBRPC dry membranes with thickness about 220 um were obtained after drying at 60 °C in a vacuum oven for 24 h. After punching into circular piece with diameter of 10 mm, the XBRPC dry membranes were activated by soaking in 1.0 M $LiPF_6$ electrolyte solution of ethylene carbonate (EC) and dimethyl carbonate (DMC) (1:1 v/v) to prepare XBRPC gel polymer electrolytes with a thickness of approximately 230μm.

Characterization

The morphology of the cross-section of XBRPC membrane was investigated using a field emission scanning electron microscope (JEOL JSM-6380LA). XBRPC membranes were broken in liquid nitrogen to obtain a cross section. A weight loss temperature value was determined with a PerkinElmer TGA/DTG 6300 at a heating rate of 10 °C min^{-1} under a nitrogen atmosphere. IR spectra were obtained with a Nicolet Magna II 550 spectrometer. The electrolyte uptake (δ) of the XBRPC membrane was calculated according to the following Eq. (1):

$$\delta = \frac{M - M_0}{M_0} \times 100 \qquad \text{Eq. (1)}$$

where, M_0 is the mass of the XBRPC dry membrane and M is the mass of the XBRPC membrane after soaking in the electrolyte. The weight of the wet membrane was determined at different soaking intervals, after removing excess electrolyte on the surface by wiping softly with a tissue paper. Mechanical stress versus strain measurement of the XBRPC membrane was performed by applying stress with a compression speed of 0.5 mm min^{-1} on a UTM4000 electronic universal testing machine (Shenzhen Suns technology stock Co. LTD).

Electrochemical Measurements

The ionic conductivity (σ) of GPEs was measured by electrochemical impedance measurements (EIS) and calculated as Eq. (2):

$$\sigma = \frac{d(cm)}{R_b(\Omega)S(cm^2)} \qquad \text{Eq. (2)}$$

where d and S denote the thickness and area of the GPE, respectively, resistance Rb can be estimated from the impedance spectra at the point where the line intercepted the real part in the high frequency region.

EIS tests were performed with Zahner Ime6ex electrochemical analyzer at amplitude of 5 mV over a frequency range of 1.0 MHz-1.0 Hz at various temperatures ranging from 293 to 353 K. The polymer electrolytes were sandwiched between two polished gold electrodes with diameter of 10 mm that acted as ion blocking electrodes in a specially designed cell setup for conductivity studies. The cell was placed into a self-designed oven coupled with a temperature controller. For each temperature, at least 20 min were waited to ensure thermal equilibration of the sample before the impedance response was recorded. Linear sweep voltammetry was performed on a stainless steel （SS） working electrode with a lithium counter electrode at a scan rate of 0.1 mV s^{-1}.

Two-electrode electrochemical coin cells were fabricated by placing the GPE between lithium metal anode and carbon-coated lithium iron phosphate ($LiFePO_4$) cathode. The commercial cathode mixture is composed of 80% $LiFePO_4$, 10% super P black, and 10% PVDF (polyvinylidene fluoride) binder coated in aluminum foil using doctor blade technique and subsequently dried in the oven at 70 °C. Before the cell assembly, composite cathode was dried in a vacuum oven at 60 °C for 12 h to remove the residual solvent traces. The test cells, Li/GPEs/$LiFePO_4$ were fabricated in 2025 coin cell and electrochemical tests were conducted using galvanostatic charge-discharge battery cycler (BTS XWJ, Neware Tech. Co.), between 2.5 and 4.0 V at room temperature at current rate of 0.1 C. The activation of XBRPC membrane to prepare GPE and the fabrication of test cells were carried out in an argon-filled glove box with oxygen and moisture level <0.1 ppm.

Results and discussion

The XBRPC membrane was fabricated by cross-linking network of PPC and BR. Fig. 1 shows the conceptual structure of the XBRPC polymeric framework. PPC chains are an important component of GPE polymeric frameworks because they effectively solvate the ion salt and serve as a solvent gelator [29-31]. The cross-linking of BR not only enhances the elasticity and mechanical strength of the XBRPC polymeric framework, but also lower the production cost of the

GPEs. Blending PEG with XBRPC precursors increases the compatibility of BR and PPC and forms composite films with homogeneous structure. PEG chains connect the BR and PPC chains by physical cross-linking to construct a 3D network.

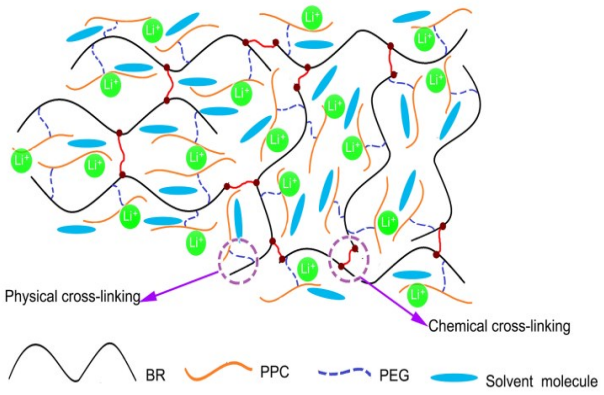

Fig. 1 Conceptual structure of the XBRPC polymeric framework

Fig. 2 shows the IR spectra of the purified BR, PPC and XBRPC70. The characteristic absorption peaks of BR shown in Fig. 2(a) are observed at 1654 cm^{-1}(C=C stretching vibration), 993 cm-1 and 910 cm^{-1} (=C-H wagging vibration in –CH=CH_2). The typical peaks of PPC shown in Fig. 2(c) are 1747cm^{-1} (stretching vibration band of C=O), 1233 $cm^{-1}$and 1069 cm^{-1} (stretching vibration band of C−O−C). In the case of XBRPC70, all the typical peaks of BR and PPC change clearly. The C=O and C=C stretching vibration peaks have shifted to lower wave numbers at 1726 cm^{-1} and 1638 cm^{-1} , respectively, with reduced relative intensity in the XBRPC70. The strong C−O−C stretching vibration of PPC, which has merged with the C−O stretching vibration of PEG to form a small shoulder and a broad band centered at 1109 cm^{-1}. The above-mentioned phenomena obviously indicate the physical cross-linking between PPC and BR in the XBRPC70. Furthermore，the =C-H wagging vibration from –CH=CH_2 in the BR main chain disappeared in the XBRPC70. This change is possibly attributable to the formation of chemical cross-linking. Since the =C-H is highly sensitive to addition reaction, the disappearance of this band is highly indicative of the presence of chemical cross-linking of BR main chain. Hence, the above analysis has confirmed the formation of a BR-interpenetrating cross-linking PPC network.

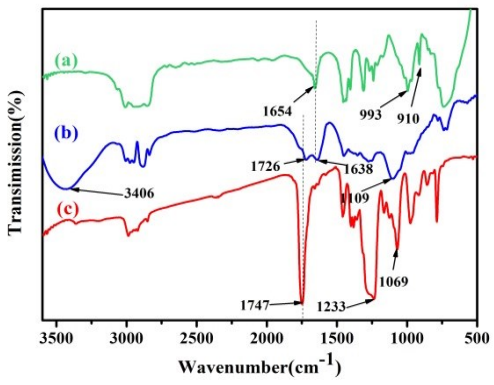

Fig. 2 FTIR spectra of the (a) BR; (b) XBRPC70 and (c) PPC at wave number range of 500-3400 cm^{-1}

Fig. 3 displays the SEM images of XBRPC50, XBRPC60, XBRPC70 and XBRPC80 membranes, respectively. It can be seen from Fig. 3(c) that the cross sections of the XBRPC50, XBRPC60, and XBRPC70 membranes are relatively homogeneous, while that of XBPRC80 is heterogeneous. Since PPC is much polar than BR, they are immiscible in essence [32]. At low BR content, the BR tends to aggregate into large particles separating from the bulk PPC, while at high BR content, the BR phase may be small and embedded within the PPC matrix. A homogeneous morphology is a highly desirable characteristic which is related to electrolyte retention [33, 34]. From what is shown in Figure 3, it can be concluded that the appropriate PPC: BR ratio is less than 80%.

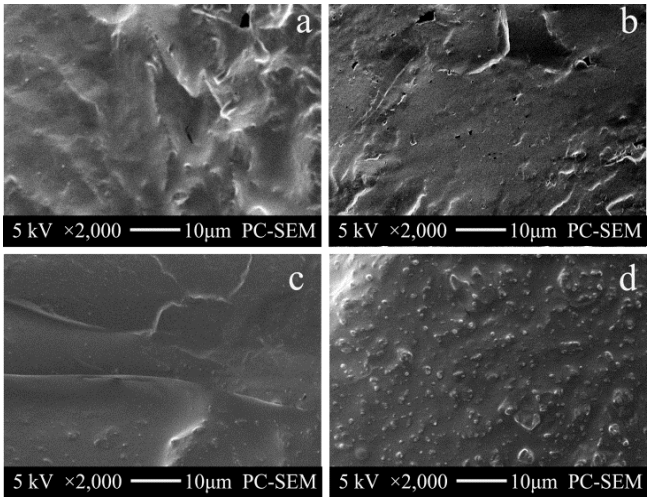

Fig. 3 SEM images of XBRPC membranes (a) XBRPC50, (b) XBRPC60, (c) XBRPC70 and (d) XBRPC80

The effect of the cross-linking between PPC and BR on the thermal stability of the XBRPC polymer membranes is studied using the thermal gravity analysis (TGA) and differential thermal analysis (DTG). Fig. 4 shows the TGA and DTG curves of pure PPC, XBRPC50, XBRPC60, XBRPC70 and XBRPC80 polymer membranes under nitrogen atmosphere, respectively. As seen in Fig. 4a, there is one weight loss for pure PPC starting at 260°C, whereas the XBRPC polymer membranes show a characteristic two step weight loss, with the first peak at a temperature 272°C and second peak at 420°C corresponding to the decomposition temperature of PPC and BR, respectively. Compared with pure PPC, the first decomposition peak of the XBRPC polymer membranes is slightly shifted to higher temperature as shown in Fig. 4a inset. This can be attributed to the cross-linking effect between PPC and BR which leads to good thermal stability. From the DTG results in Fig. 4b, it can be seen that the curves of the XBRPC polymer membranes become coarser and wider than that of pure PPC. The addition of BR would enhance their thermal stability by acting as a superior supporter. The BR which disperses in matrix leads to the difficulty in heat conduction and acts as a mass transport barrier to the volatile products which generate during the first thermal decomposition. These functions of BR will result in the lag, wide and coarse peaks of the XBRPC polymer membranes during decomposition.

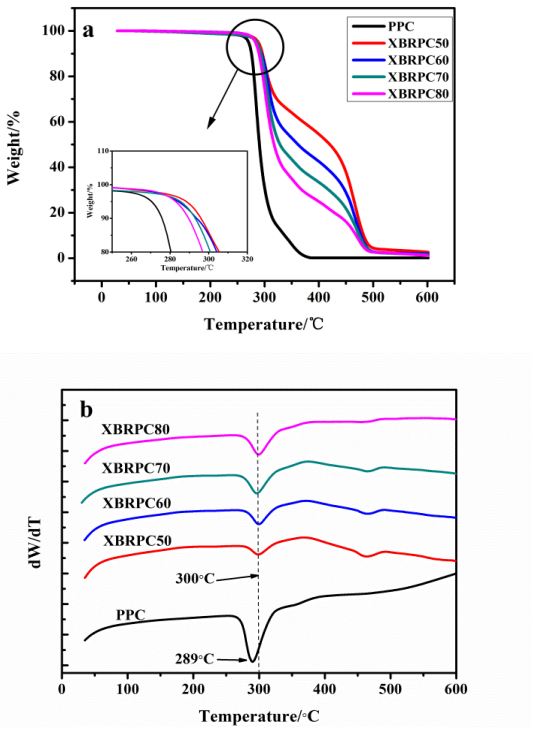

Fig. 4 TGA (a) and DTG (b) curves of pure PPC, XBRPC50, XBRPC60, XBRPC70 and XBRPC80 membranes. The inset image is the enlarged TGA curves

The content of PPC and the stability of XBRPC polymeric framework result in different electrolyte retention. The electrolyte uptake amounts of the XBRPC50, XBRPC60, XBRPC70 and XBRPC80 membranes can reach 120,124, 135 and 119 wt %, respectively. It is clear that the electrolyte uptake amounts of the XBRPC50, XBRPC60 and XBRPC70 membranes increase with increasing the content of PPC in the polymer matrix. It reveals that the amount of organic electrolyte is closely related to the content of PPC in the polymer matrix and the property of XBRPC polymeric framework. While the morphologies of XBRPC50 and XBRPC 80 are quite different, they exhibit similar electrolyte uptake. This implies that the morphology of membranes is not the only factor influencing electrolyte uptake. Generally, these electrolyte uptakes are in the most appropriate region for polymer electrolytes.

TGA curves for equal weights of XBRPC membranes soaked with the same amount of electrolyte were obtained, as shown in Fig. 5. The emission of large amounts of combustible gases at temperatures below 120 °C is the primary reason for lithium-ion battery accidents such as fires and explosions [35]. The weight loss of the series of XBRPC membranes is less than 15% at 120 °C, which means the evaporation of organic gases for the XBRPC membranes is below 15%.The result is lower than the commercial Celgard M824 separator [13], indicating better stability. This property of slow emission of organic gases greatly improves the safety of lithium-ion battery. In addition, the proposed membrane also endows lithium-ion battery with good electrochemical performance and is mainly contributed by the superior electrolyte retention ability of XBRPC at high temperature.

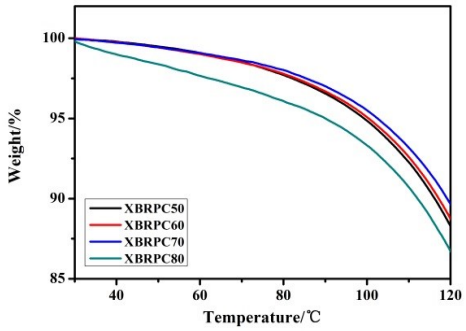

Fig. 5 TGA curves for equal weights of XBRPC membranes soaked with the same amount of electrolyte

A good mechanical property of GPE plays an important role in preventing a short circuit, which results in the positive and negative contacts, during application of lithium-ion batteries. The stress-strain curves of the XBRPC membranes are shown in Fig. 6(a). The maximum stress of the XBRPC50, XBRPC60, XBRPC70 and XBRPC80 membranes are 4.50, 3.95, 3.91 and 3.38 MPa, respectively. This phenomenon could be explained as follows: The addition of BR increases the stress of the XBRPC membranes while the homogeneous and symphysic morphology is beneficial for further improving the mechanical property of the polymer membranes. Besides, as shown in Fig. 6(b), the polymer membranes exhibit excellent dimensional stability, mechanical strength and elasticity when the XBRPC70 sample trapping 135wt% liquid electrolyte. The results indicate that, with a low BR level of 30wt%, XBRPC70 film is robust, self-standing and flexible with no liquid flow, which can meet the requirement for practical applications.

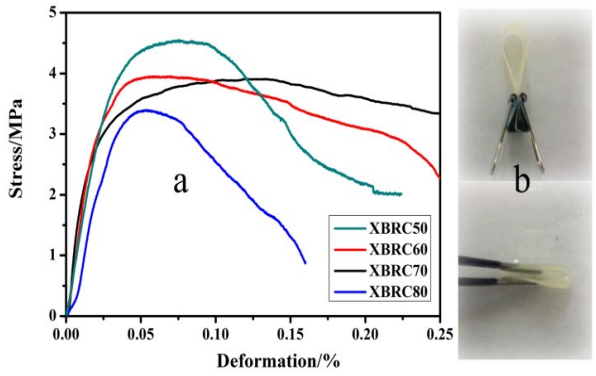

Fig. 6 (a) Stress-strain curves of XBRPC membranes; (b) Digital images of self-standing film of XBRPC70 membrane and XBRPC70 GPE membrane

The EIS method was carried out to analyze the ionic conductivity of the GPEs. Impedance spectra of the XBRPC GPEs are shown in Fig. 7(a). The impedance spectra of all XBRPC GPEs are almost linear along with the real x-axis. The disappearance of semicircular portion in the high frequency range suggests that the current carriers are ions according to theoretical analysis [36]. Fig. 7(b) shows the ionic conductivity data of all XBRPC GPEs at room temperature which is calculated from the impedance plots. The ionic conductivity of the XBRPC50, XBRPC60, XBRPC70 and XBRPC80 GPEs are 0.45 mS cm^{-1}, 0.62 mS cm^{-1}, 1.25 mS cm^{-1} and 0.56 mS cm^{-1}, respectively. The ionic conductivity follows the

same trend as the electrolyte uptake. High electrolyte uptake leads to strong ionic conductivity. There are several contrasting factors that affect the ionic conductivity of the electrolyte solutions [37]. The dielectric constants of the carbonate solvents are not high enough to effectively solvate ion pairs for swift ion motion [38]. Hence, the C-O-C chains in the GPE have played an important role in solvating the ion salt to increase the ionic conductivity [39-40]. The ion conduction of GPE may occur through the free volume phase in the polymeric framework or through the swollen polymer chain phase [41]. It means that high ion conductivity of GPE is also caused by the high degree of $LiPF_6$ dissociation by the ether-oxygen atom and the segregated XBRPC framework, which forms more ionic transport channels after swelling, by absorbing organic electrolyte [42-43]. Meanwhile, the solvent molecules reduce the Li^+ complexation degree with the oxygen atom, increasing the segmental mobility of the polymer [9]. In general, the combined action of high electrolyte retention, great degree of $LiPF_6$ dissociation and stable polymeric frame work can result in a high ionic conductivity of GPE.

The typical plot of ionic conductivity versus inverse temperature (1000/T) for XBRPC gel polymer electrolyte with different ratio of BR and PPC is depicted in Fig. 7(c). In general, the ionic conductivities of all samples increase with the increase of temperature, obeying the Arrhenius plot of conductivity, which suggests that the conductivity is thermally activated. At 353K, the ionic conductivity of the XBRPC50, XBRPC60, XBRPC70 and XBRPC80 GPEs are 0.93 mS cm^{-1}, 1.78 mS cm^{-1}, 3.51 mS cm^{-1} and 1.04 mS cm^{-1}, respectively. This may be result from that intense polymer chain motion and relaxtion at high temperature. The activation energies for the movement of ions are 18.99，18.92，18.17 and 19.20 kJ mol^{-1}, respectively, for the XBRPC50, XBRPC60, XBRPC70 and XBRPC80 GPEs. The electrolyte retention is a key factor of activation energy. The electrolyte uptake amount of the XBRPC70 is very high because of the high content of PPC and the excellent stability of XBRPC polymeric framework. The movement of ions in the XBRPC70 GPE is easier than that in the other BR/PPC based GPEs. As a result, the activation energy of the XBRPC70 GPE is lower than that of the other XBRPC based GPEs. In general, for GPEs with different ratios of PPC and BR, the amount of PPC is an effective factor in improving ionic conductivity.

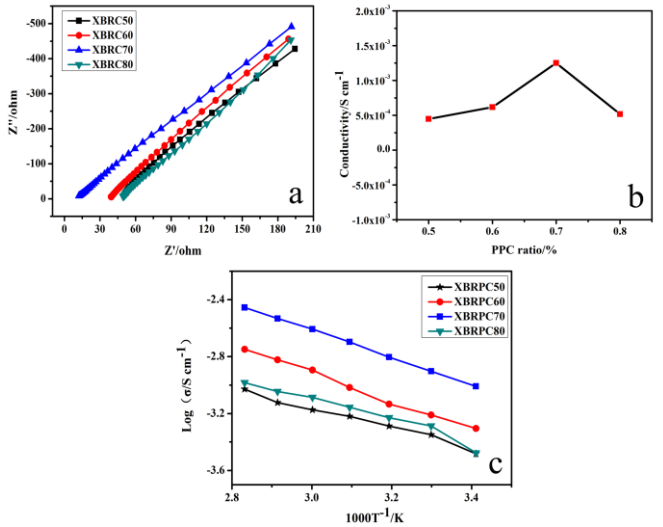

Fig. 7 (a) Impedance plots of the XBRPC GPEs at room temperature; (b) The ionic conductivity of the XBRPC GPEs ; (c) Typical plot of ionic conductivity versus inverse temperature (1000/T) for the XBRPC GPEs from 20°C to 80 °C.

The electrochemical stability window of the energy storage device provides essential information for assessing the success. For determining the electrochemical stability window of the GPEs, a linear sweep voltammetry (LSV) experiment was carried out in the potential range of 2.5–6.0V (vs. Li^+/Li) at a scan rate of 0.5 mV s^{-1}as shown in Fig.8. The LSV curves of the XBRPC50, XBRPC60 and XBRPC80 GPEs with an electrochemical stability ranged from 4.1V to 4.3 V, whereas the XBRPC70 produced a larger range of about 4.5V. This characteristic is influenced by the dynamic formation of Li passivation layer between solvent molecules (EC and DMC) at the Li electrode [12]. The results show that the cross-linking of BR can increase the stability of XBRPC film and PPC is beneficial to trap liquid electrolytes through good compatibility between carbonate solvent molecules in electrolyte and ester group on the main chain of PPC. It might be speculated that the electrolyte retention plays an important role at the electrode/electrolyte interface. Consequently, the electrochemical window stability of the GPE film improves, which makes it suitable for the application in lithium ion batteries.

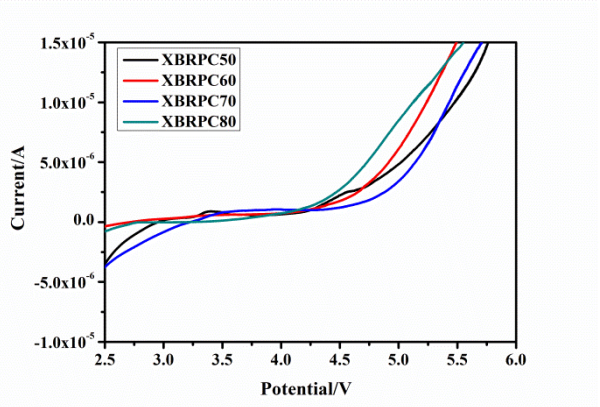

Fig. 8 Electrochemical windows for XBRPC membranes

To evaluate the electrochemical performance of the XBRPC GPEs, the cells were assembled with XBRPC GPEs sandwiched between $LiFePO_4$ cathode and a lithium metal anode. Fig. 9(a) presents the initial discharge curves of the Li/ XBRPC GPEs/$LiFePO_4$ cells using XBRPC GPEs at rate of 0.1 C in voltage range of 2.5-4.0V at room temperature. As seen in Fig.9(a), the Li/ XBRPC70 GPE / $LiFePO_4$ cell delivered the initial discharge capacity of 119 $mAhg^{-1}$, which is 71% of the theoretical capacity of $LiFePO_4$ (170 $mAhg^{-1}$) [44] ,but higher than the cells with XBRPC50 (86 $mAhg^{-1}$), XBRPC60 (108 $mAhg^{-1}$) and XBRPC80 (79 $mAhg^{-1}$) GPEs. This is possibly attributed to the higher ionic conductivity of XBRPC70 GPE, which benefit to improve the lithium ion transportation. However, lower discharge capacity is due to weaker interaction between XBRPC polymer electrolyte film and electrodes without infiltrating electrolyte into the whole cathode mixture [12].Cycle performance of the Li/ XBRPC70 GPE / $LiFePO_4$ cell at 0.1 C for 70 cycles was shown in Fig. 9(b). The cell delivered discharge capacity of 100 mAh g^{-1} after 70 cycles. The columbic efficiency is closed to 98% with a very low level of capacity recession, which show that the cell using XBRPC70 GPEs has excellent reversible cycle performance and battery stability. From these results, it can be concluded that the XBRPC70 based gel polymer electrolyte has a potential for the use in Lithium-ion polymer battery. However, for practical application of this polymer electrolyte, much more

attention should be paid to the interfacial adhesion between polymer electrolyte film and electrodes in further research.

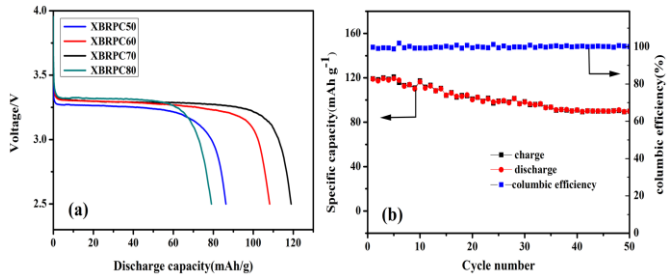

Fig. 9 (a) The initial discharge curves of Li/ XBRPC70 GPE / $LiFePO_4$ cells at 0.1 C and 2.5–4.0V; (b) Cycling performances of Li/ XBRPC70 GPE/$LiFePO_4$ cell

Conclusions

In summary, a novel series of gel polymer electrolytes by incorporating PPC with BR through building a BR-interpenetrating cross-linking PPC network have been synthesized. The XBRPC70 polymeric framework is highly homogeneous and stable, results in excellent electrolyte retention, higher ionic conductivity, low emission of combustible gases and outstanding mechanical property. The high ionic conductivity of the XBRPC70 GPE can be contributed to:(1) The proper content of PPC ensures high electrolyte retention ability, (2) the C-O-C chains in the XBRPC70 contributes to solvating the ion salt, (3) BR cross-linking segments provide the XBRPC70 with excellent stability. Moreover, the ionic conductivities of all XBRPC samples increase with the increase of temperature, obeying the Arrhenius plot of conductivity. Electrochemical stability window of XBRPC GPE was above 4.5 V versus Li^+/Li. Li/ XBRPC70 GPE / $LiFePO_4$ battery delivered an initial discharge capacity of 119 mAh $g^{-1}$and 100 mAh g^{-1} after 70 cycles at 0.1C with excellent cycle performance. These results demonstrate that the XBRPC70 based gel polymer electrolyte has a potential for the use in Lithium-ion polymer battery.

Acknowledgements

This research was supported financially by the Guangdong Natural Science Foundation (Grant No. 9151064201000039), the Guangdong Science and Technology Planning Project (No.2009B010900025), the National Natural Science Foundation of China (Nos. 51003034 and 21173088), the Key Academic Program of the 3rd phase '211 Project' (No. 2009B010100001), and the State Key Laboratory of Motor Vehicle Biofuel Technology (No. 2013025).

Notes and references

1 M. Armand and J. M. Tarascon, *Nature*, 2008, **451**, 652-657.
2 P. Yang, P. Zhang, C. Shi, L. Chen, J. Dai and J. Zhao, *J Membrane Sci*, 2015, **474**, 148-155.
3 M. Rao, X. Geng, Y. Liao, S. Hu and W. Li, *J Membrane Sci*, 2012, **399-40**0, 37-42.
4 L. H. Saw, Y. Ye and A. A. O. Tay, *Appl Energ*, 2014, **131**, 97-107.
5 Y. S. Choi and D. M. Kang, *J Power Sources*, 2014, **270**, 273-280.
6 Y. Lee, J. H. Lee, J. Choi, W. Y. Yoon and D. Kim, *Adv Funct Mater*, 2013, **23**, 1019-1027.
7 M. Patel, M. Gnanavel and A. J. Bhattacharyya, *J Mater Chem*, 2011, **21**, 17419.
8 F. Wu, G. Tan, R. Chen, L. Li, J. Xiang and Y. Zheng, *Adv Mater*, 2011, **23**, 5081-5085.
9 Q. Wang, P. Ping, X. Zhao, G. Chu, J. Sun and C. Chen, *J Power Sources*, 2012, **208**, 210-224.
10 F. Croce, G. B. Appetecchi, L. Persi and B. Scrosati, *Nature*, 1998, **394**, 456-458.
11 S. Wang, S. Hou, P. Kuo and H. Teng, *Acs Appl Mater Inter,* 2013, **5**, 8477-8485.
12 A. M. M. Ali, R. H. Y. Subban, H. Bahron, M. Z. A. Yahya and A. S. Kamisan, *J Power Sources*, 2013, **244**, 636-640.
13 P. Kuo, C. Wu, C. Lu, C. Tsao, C. Hsu and S. Hou, *A Acs Appl Mater Inter,* 2014, **6**, 3156-3162.
14 J. W. Fergus, J Power Sources, 2010, **195**, 4554-4569.
15 H. Li, H. Zhang, Z. Liang, Y. Chen, B. Zhu and L. Zhu, *Electrochim Acta*, 2014, **116**, 413-420.
16 R. Prasanth, N. Shubha, H. H. Hng and M. Srinivasan, *J Power Sources*, 2014, **245**, 283-291.
17 J. R. Kim, S. W. Choi, S. M. Jo, W. S. Lee and B. C. Kim, *Electrochim Acta*, 2004, **50**, 69-75.
18 J. Zhang, S. Chen, X. Xie, K. Kretschmer, X. Huang, B. Sun and G. Wang, *J Membrane Sci*, 2014, **472**, 133-140.
19 S. Ferrari, E. Quartarone, P. Mustarelli, A. Magistris, M. Fagnoni, S. Protti, C. Gerbaldi and A. Spinella, *J Power Sources*, 2010, **195**, 559-566..
20 N. Wu, Q. Cao, X. Wang, X. Li and H. Deng, *J Power Sources*, 2011, **196**, 8638-8643.
21 M. Rao, X. Geng, Y. Liao, S. Hu and W. Li, *J Membrane Sci*, 2012, **399-400**, 37-42.
22 Q. Xiao, Z. Li, D. Gao and H. Zhang, *J Membrane Sci*, 2009, **326**, 260-264.
23 X. Yu, M. Xiao, S. Wang, Q. Zhao and Y. Meng, *J Appl Polym Sci*, 2010, **115**, 2718-2722.
24 X. Yu, M. Xiao, S. Wang, D. Han and Y. Meng, *J Appl Polym Sci*, 2010, **118**, 2078-2083.
25 X. L. Lu, F. G. Du, X. C. Ge, M. Xiao and Y. Z. Meng, *J Biomed Mater Res A*, 2006, **77A**, 653-658.
26 S. Arai, Y. Suwa, M. Endo, *J Electrochem Soc*, 2011, **158**, 49-53.
27 J. Song, M. Zhou, R. Yi, T. Xu, M.L. Gordin, D. Tang, Z. Yu, M. Regula, D. Wang, *Adv Funct Mater*, 2014, **24**,5904-5910.
28 S. Komaba, K. Shimomura, N. Yabuuchi, T. Ozeki, H. Yui, K. Konno, *J. Phys Chem. C*, 2011, **115**, 13487-13495.
29 D. Zhou, R. Zhou, C. Chen, W. Yee, J. Kong, G. Ding, X. Lu, *J. Phys Chem. B*, 2013,**117**,7783-7789.
30 Y.J. Choi, Y. Han, M. Ok, D. Kim, *Macromol Chem Phys*, 2011, **212**, 2583-2588.
31 G.P. Dukhanin, A.N. Gaidadin, I.A. Novakov, *Russ J Appl Chem*, 2014, **87**, 1868-1871.
32 A. Bandyopadhyay, V. Thakur, S. Pradhan and A. K. Bhowmick, *J Appl Polym Sci*, 2010, **115**, 1237-1246.
33 C. Gerbaldi, J.R. Nair, S. Ferrari, A. Chiappone, G. Meligrana, S. Zanarini, P. Mustarelli, N. Penazzi, R. Bongiovanni, *J Membrane Sci*, 2012, **423-424**, 459-467.
34 Jr. D.T. Hallinan, N.P. Balsara, *Annu Rev Mater Res*, 2013, 43, 503–525.
35 Y. Zhu, F. Wang, L. Liu, S. Xiao, Z. Chang and Y. Wu, *Energ Environ Sci*, 2013, **6**, 618.
36 J.R. Macdonald, *J Chem Phys*, 1974, **61**, 3977.
37 R. Prasanth, N. Shubha, H. H. Hng and M. Srinivasan, *J Power Sources*, 2014, **245**, 283-291.
38 M. Winter and R. J. Brodd, *Chem Rev*, 2004, **104**, 4245-4270.
39 D.E. Fenton, J.M. Parker and P.V. Wright, *Polymer*, 1973, **14**, 589.
40 W. H. Meyer, Advanced materials (Deerfield Beach, Fla.), 1998, 10, 439.
41 J. Saunier, F. Alloin, J. Y. Sanchez and G. Caillon, *J Power Sources*, 2003, **119-121**, 454-459.
42 M. M. Rao, J. S. Liu, W. S. Li, Y. Liang and D. Y. Zhou, *J Membrane Sci*, 2008, 322, 314-319.
43 P. Carol, P. Ramakrishnan, B. John and G. Cheruvally, *J Power Sources*, 2011, **196**, 10156-10162.
44 S. Chung, J. T. Bloking and Y. Chiang, *Nat Mater*, 2002, **1**, 123-128.

Graphical Abstract

Novel polybutadiene rubber interpenetrating cross-linking poly (propylene carbonate) network has been synthesized as GPEs with excellent electrochemical performances for lithium-ion batteries.